Electronic Supplementary Material (ESI) for Physical Chemistry Chemical Physics.

Supporting information

Tuning the properties of visible-light-responsive tantalum (oxy)nitride photocatalysts by non-stoichiometric compositions: a first-principle viewpoint

Moussab Harb,*[,a] Philippe Sautet,[b] Ela Nurlaela,[a] Pascal Raybaud,[c] Luigi Cavallo,[a] Kazunari Domen,[d] Jean-Marie Basset[a] and Kazuhiro Takanabe*[,a]

[a] KAUST Catalysis Center (KCC), King Abdullah University of Science and Technology (KAUST), 4700 KAUST, Thuwal 23955-6900, Kingdom of Saudi Arabia

[b] Université de Lyon, CNRS, Ecole Normale Supérieure de Lyon, Laboratoire de Chimie, 46 allée d'Italie, 69364 Lyon cedex 07, France

[c] IFP Energies Nouvelles, Rond-point de l'échangeur de Solaize, BP 3-69360 Solaize, France

[d] Department of Chemical System Engineering, The University of Tokyo, 7-3-1 Hongo, Bunkyo-ku, Tokyo, 113-8656, Japan

* Corresponding author: E-mail: moussab.harb@kaust.edu.sa
kazuhiro.takanabe@kaust.edu.sa

* Contact author: Dr. Moussab Harb, Phone: +966.2.808.07.88. Fax: +966.2.802.12.72.
E-mail: moussab.harb@kaust.edu.sa.

Electronic density of states and averaged electrostatic potential calculated using the DFT-HSE06 method for TaON and pure Ta_3N_5 slab models

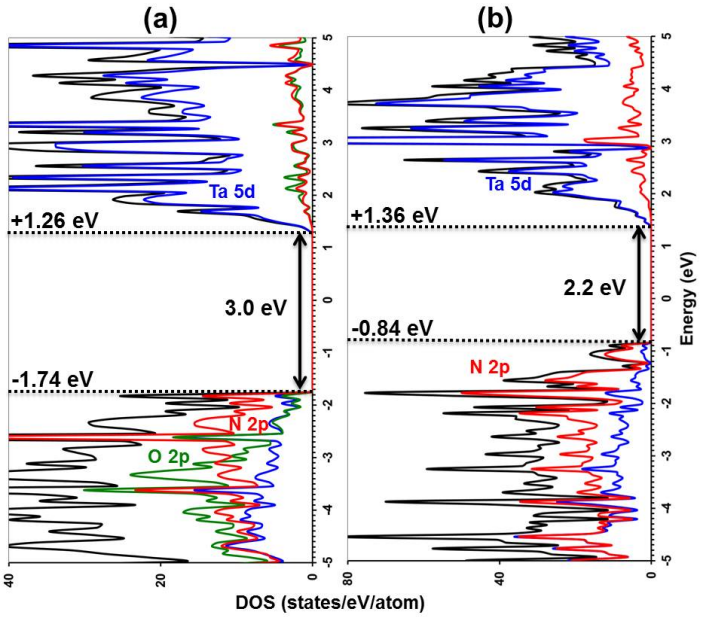

Figure S1. Electronic density of states (DOS) calculated using the DFT-HSE06 method for the two slab models reported in Figure 1: (a) TaON and (b) pure Ta_3N_5. The band gaps of the bulk materials were well reproduced. Color legend: total DOS, black; projected DOS on sub-surface Ta, blue; on sub-surface O, green; on sub-surface N, red. The values near the black dashed horizontal lines indicate E_{VB}^{slab} and E_{CB}^{slab}.

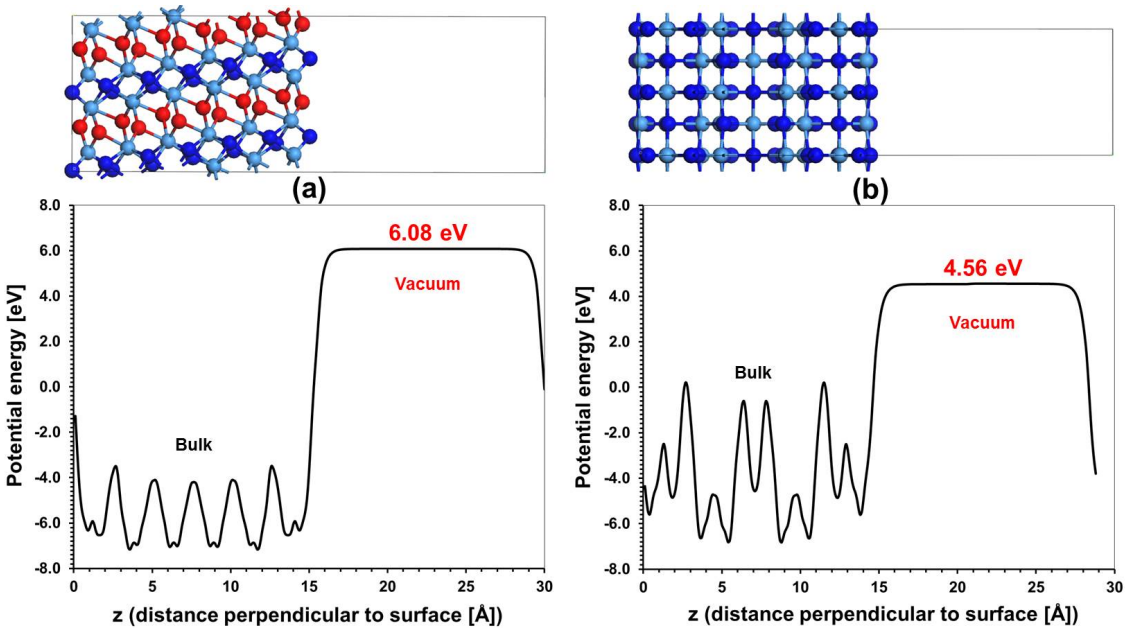

Figure S2. Schematic representation of $(2\vec{a} \times 1\vec{b})$ slab model oriented along the z-direction (top) and the corresponding profile of the electrostatic potential averaged over planes parallel to the surface (bottom), calculated using the DFT-HSE06 method for (a) TaON and (b) pure Ta_3N_5. The values in red indicate E_{VAC}.

Scanning electron micrographs and X-ray diffraction patterns for the prepared Ta_2O_5, TaON and Ta_3N_5 samples

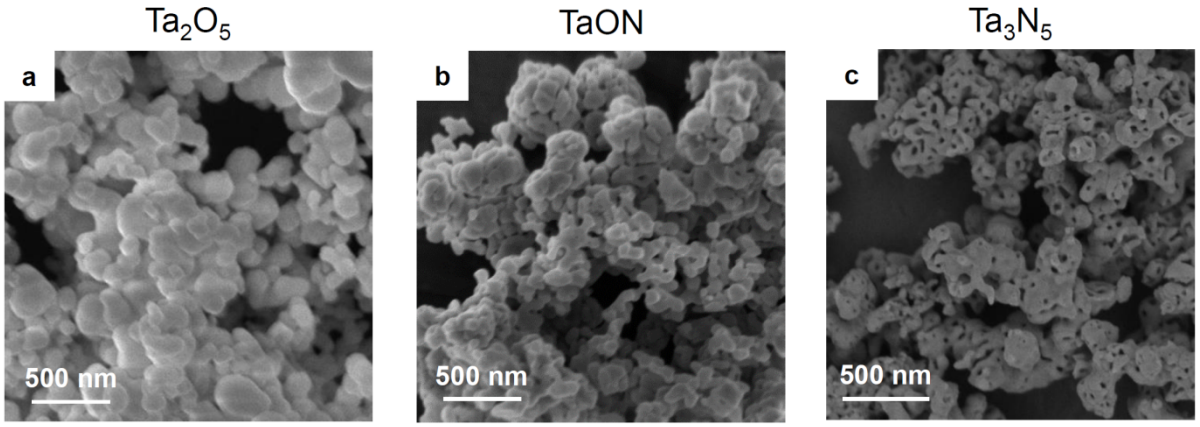

Figure S3. SEM images for prepared Ta_2O_5, TaON and Ta_3N_5 samples.

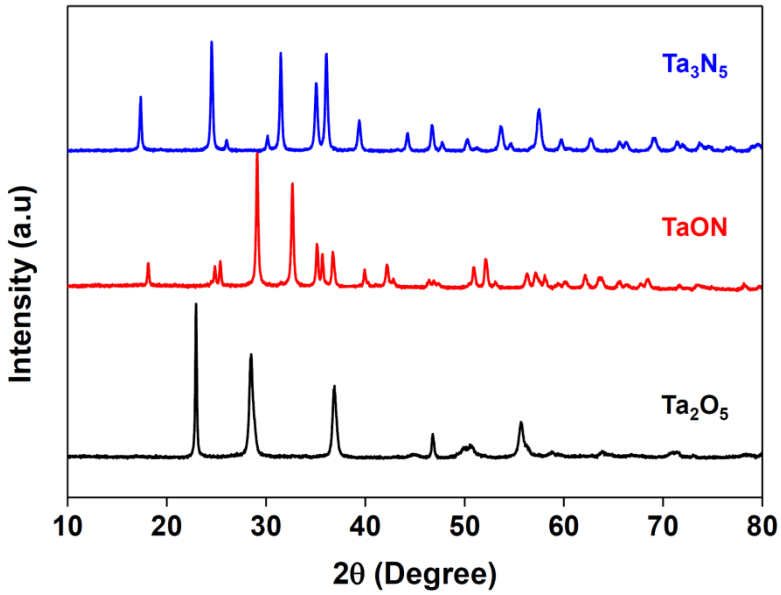

Figure S4. XRD patterns for prepared Ta_2O_5, TaON, and Ta_3N_5 samples

DFT-optimized metastable structures and relative energies (in brackets) obtained using the DFT-PBE method for $TaO_{0.90}N_{1.06}$ and $Ta_{2.91}N_{4.58}O_{0.41}$ materials

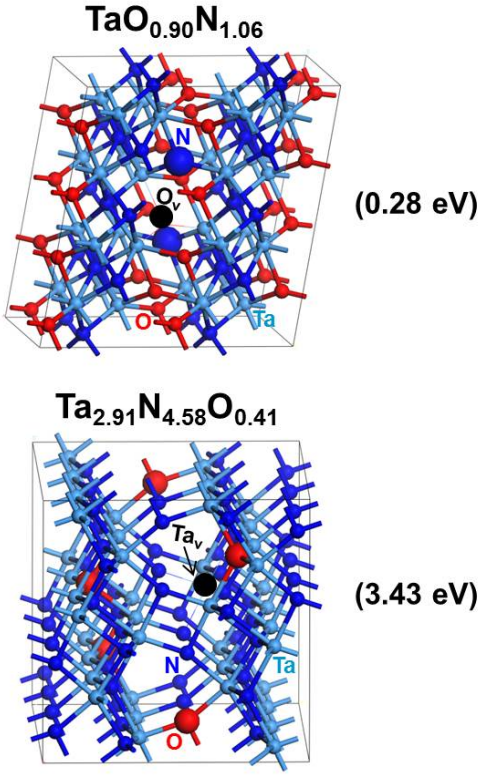

Figure S5. DFT-optimized metastable structures and relative energies (in brackets) obtained using the DFT-PBE method for $TaO_{0.90}N_{1.06}$ and $Ta_{2.91}N_{4.58}O_{0.41}$.

DFT-optimized lowest-energy and metastable structures together with the relative energies (in brackets) and lattice parameters obtained using the DFT-PBE method for $Ta_3N_{4.83}O_{0.25}$ material

For $Ta_3N_{4.83}O_{0.25}$ obtained by replacing two N atoms with two O atoms and by inserting one additional O atom into the 96-atom orthorhombic Ta_3N_5 supercell, the structure is particularly stable when the three O atoms are gathered between two Ta atoms, forming two TaO_3N_4 polyhedra, one TaO_2N_5 polyhedron and one $TaON_5$ octahedron (see structure (a) below). The lattice parameters obtained for this structure are also very similar to the lattice parameters of pure Ta_3N_5, except for a slight decrease in the angle α, by 0.32° (see the Table below). In this structure, the interstitial O atom is located 2.22 and 2.73 Å from the two other substitutional O atoms, occupying two three-coordinated N atoms bridging between two Ta atoms. The most stable spin configuration is a singlet state, leading formally to three O^{2-} defects replacing two N^{3-} species. Another structural configuration with two O atoms substituting for two four-coordinated N atoms separated by 4.55 Å and one interstitial O atom located at 2.34 Å from

each one was found to be 1.37 eV higher than the lowest-energy structure (see structure (b) below).

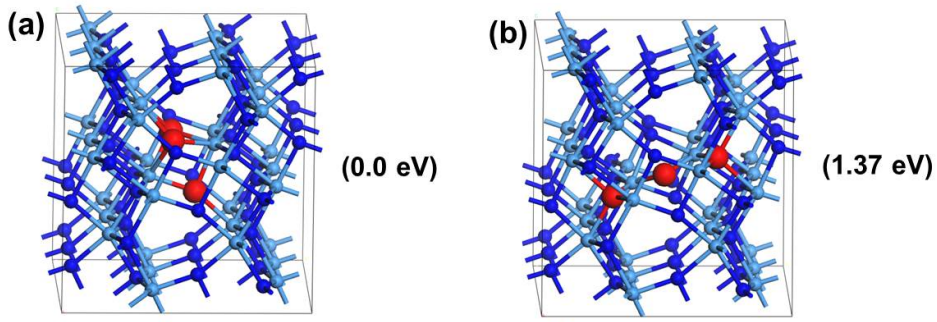

structure	lattice parameters					
	a (Å)	b (Å)	c (Å)	α (°)	β (°)	γ (°)
(a)	3.895	10.237	10.250	89.68	90	90

Figure S6. DFT-optimized lowest-energy and metastable structures together with the relative energies (in brackets) and lattice parameters obtained using the DFT-PBE method for $Ta_3N_{4.83}O_{0.25}$.

Electronic density of states calculated using the DFT-PBE method for bulk TaON and pure Ta_3N_5 materials

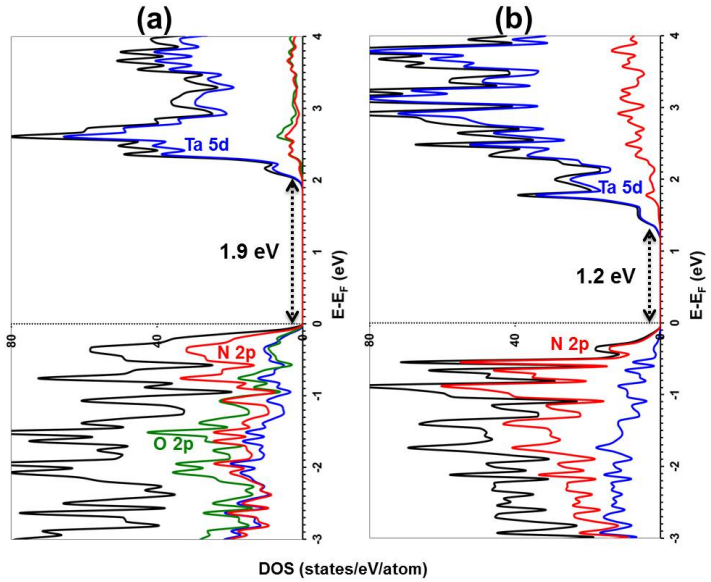

Figure S7. Electronic density of states (DOS) calculated using the DFT-PBE method for (a) TaON and (b) pure Ta_3N_5. Color legend: total DOS, black; projected DOS on Ta, blue; on O, green; on N, red. The black dashed horizontal lines indicate the top part of the valence bands.

Electronic density of states and UV-Vis optical absorption spectrum calculated using the DFT (DFPT)-HSE06 methods for bulk $Ta_3N_{4.83}O_{0.25}$ material

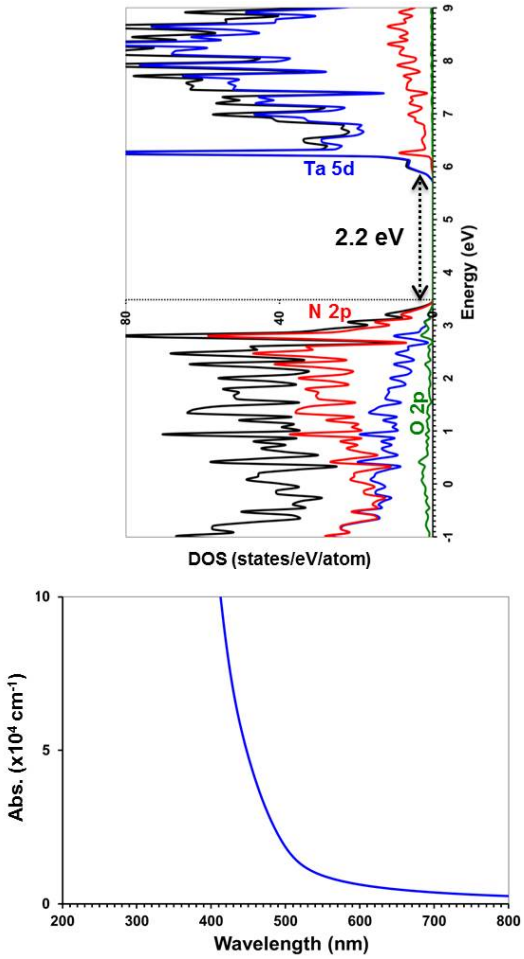

Figure S8. Electronic density of states (DOS) and UV-Vis optical absorption spectra calculated using HSE06 for $Ta_3N_{4.83}O_{0.25}$. Color legend: total DOS, black; projected DOS on Ta, blue; on O, green; on N, red. The black dashed horizontal lines indicate the top part of the valence bands.

Cyclic voltammograms and Mott-Schottky plots for the prepared TaON and Ta_3N_5 samples

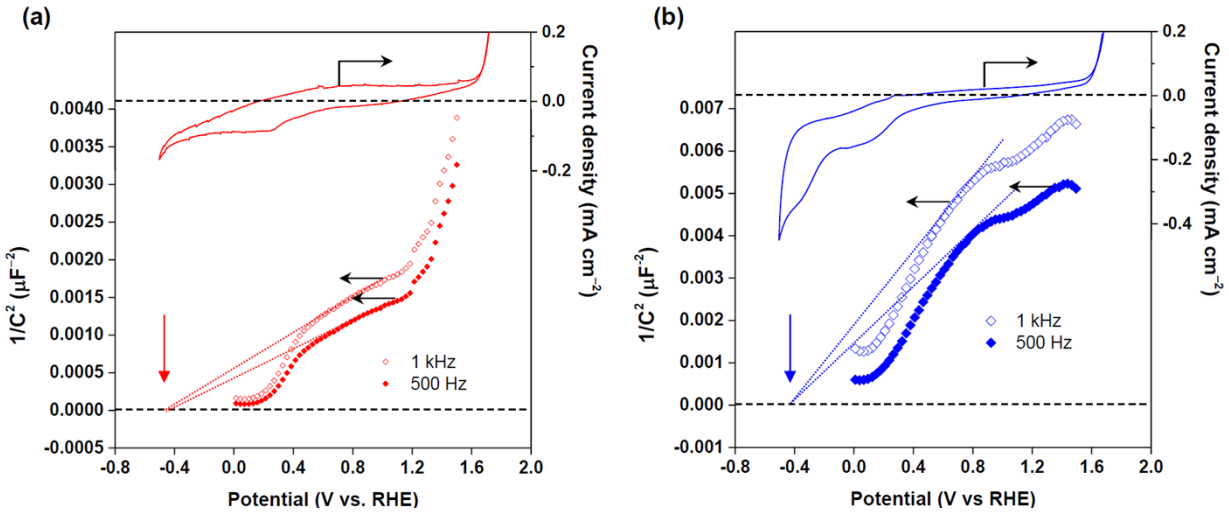

Figure S9. Cyclic voltammetry and Mott-Schottky plots for (a) TaON and (b) Ta_3N_5 (1 M NaOH aq., 50 mV s^{-1}, 298 K).

Band edge positions predicted by the DFT-HSE06 method for $Ta_3N_{4.83}O_{0.25}$ material

For $Ta_3N_{4.83}O_{0.25}$, both the valence and conduction band edge positions are shifted upward by 0.1 eV as compared with pure Ta_3N_5 (i.e., 0.4 eV and 1.4 eV above the O_2/H_2O and H^+/H_2 levels, respectively); therefore, its ability to oxidize water is even worse.

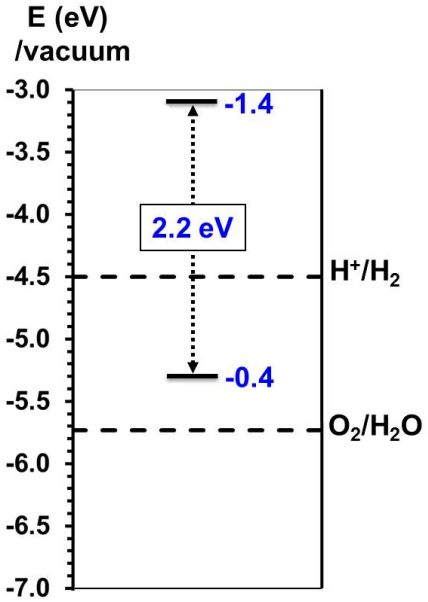

Figure S10. Valence and conduction band edge positions predicted by the DFT-HSE06 method for $Ta_3N_{4.83}O_{0.25}$. The values are given with respect to vacuum level (in eV).